Stress Sensitivity of the T(0,1) mode velocity for cylindrical waveguides

Jabid Quiroga Mendez, Octavio Andrés González Estrada, Yesid Rueda Ordonez

Stress Sensitivity of the T(0,1) mode velocity for cylindrical waveguides

Jabid Quiroga[†,a], Octavio Andres Gonzalez-Estrada[⋆,b], and Yesid Rueda Ordonez[‡]

[†,a]GIEMA, School of Mechanical Engineering, Universidad Industrial de Santander, Ciudad Universitaria, Bucaramanga, Colombia, jabib@uis.edu.co, yjruedao@uis.edu.co

[⋆]GIC, School of Mechanical Engineering, Universidad Industrial de Santander, Ciudad Universitaria, Bucaramanga, Colombia. Orcid: 0000-0002-2778-3389, agonzale@uis.edu.co

Abstract. In this paper, the stress influence in the guided wave velocity of the fundamental torsional mode is presented. Two analytical models, based on the Acoustoelasticity effect, to compute the fundamental torsional mode velocity propagating in a specimen subject to an axial stress are studied. These models are obtained due to the relation between the $T(0,1)$ guided wave velocity and the bulk shear velocity. The analytical models to calculate the guided wave velocity are functions of the stress, second and third order elastic constants. A series of axial stress levels applied to a cylindrical waveguide is investigated with numerical simulations (Finite Elements) to estimate variations of the $T(0,1)$ guided wave velocity. This analysis provides a criterion to evaluate the practical implementation of a stress monitoring scheme based on velocity variations of the fundamental torsional mode.

Keywords: Torsional guided waves, Stressed cylinders, phase velocity, stress monitoring

1 Introduction

Lately, guided waves are gaining the attention of the NDT and SHM community. Guided waves are suitable to explore large material volume for long distances from one probe position. all material discontinuity (notches, cracks, erosion, etc) is revealed on the wave field once the ultrasonic pulse interacts with the material disturbance. The ultrasonic guided wave analysis allow the inspection of buried and underwater structures, coated structures, and structures encapsulated in insulation and concrete. Inspection of tubes and pipelines by guided waves is probable the most popular application of this technique. However, in order to have success in pipe inspection, a deep understanding of the technique is required. Several factors may affect the guided wave propagation such as environmental conditions, material structure and the presence of stress in the waveguide. Stressed media as predicted by the Acoustoelasticity effect produces velocity variations in the bulk wave, longitudinal and transversal, and consequently in the guided waves generated by them.

The stress influence in guided waves have been tackled in several studies, the change in the guided wave velocity has been used to stress monitoring in plates with biaxial loads [1], in bolts to verify tightening [2], in rails [3],[4],[5], steel strands [6],[7],[8], in grouted tendons [9] and finally in pipes [10]. Among guided waves families of modes that propagate in cylindrical structures i.e. longitudinal, flexural and torsional, the latter is preferred in some inspections. Torsional guided waves barely are affected by fluids inside or outside of the cylinder, so the energy leakage from the waveguide to the fluid is minimal because of the shearing nature of this type of guided wave. In addition, the fundamental torsional mode $T(0,1)$ is non-dispersive i.e. phase and group velocities are frequency independent and equal. Finally, due to the axisymmetric character of $T(0,1)$ the wavefield energy is distributed uniformly over the cross-section avoiding blind zones to the ultrasonic exploration.

two analytical models to compute the phase velocity of the $T(0,1)$ mode propagating in a specimen subject to an axial stress are studied based on the acoustoelasticity effect. A series of FEM simulations are performed to study the propagation of torsional guided waves in presence of stress in the waveguide.

1.1 Fundamental torsional guided waves in cylindrical waveguides

A simplified analytical model of torsional guided waves assumes that the hollow cylindrical system is geometrically axisymmetric, infinitely long, and stress-free in the boundaries. The material is

elastic, homogeneous and isotropic. The waves will be assumed to be continuous, the frequency real (steady state), and the energy is finite and constant. The solutions to motion equation will only be sought explored for guided waves, which are propagated axially.

The torsional modes are characterized mainly by a displacement primarily in the θ-direction. The axisymmetric torsional mode corresponds to an uniform azimuthal displacement in θ-direction (angular displacement) of the entire cylindrical waveguide.

The generalized guided wave propagation model is based on the combination of Euler's equation of motion and the generalized Hooke's law. Both relations yield the Navier's displacement equation of motion given by

$$(\lambda + 2\mu)\,\nabla\,(\nabla \cdot u) + \mu\nabla \times (\nabla \times u) = \rho\left(\frac{\partial^2 u}{\partial t^2}\right), \tag{1}$$

where u is the displacement vector, ρ is the mass density per unit volume and λ, μ are the Lame's constants. The resulting Navier's equations, where $(\lambda + 2\mu)\,\nabla\,(\nabla \cdot u)$ considers the dilatation (compressional) portion and, $\mu\nabla \times (\nabla \times u)$ the rotational (equivoluminal) portion of the model. These two terms are decoupled by the Helmholtz decomposition and individually belong to a wave equation of the scalar field Φ and the H vector field are written as:

$$C_1\nabla^2\Phi = \frac{\partial^2\Phi}{\partial t^2}, \tag{2}$$

$$C_2\nabla^2 H = \frac{\partial^2 H}{\partial t^2}, \tag{3}$$

where C_1 and C_2 are the longitudinal and shear bulk velocities respectively. Since Equation (1) is separable in cylindrical coordinates, the solution may be divided into the product of functions of each one of the spatial dimensions in cylindrical coordinates. Assuming no propagation in the radial direction (r) and the displacement field without variation in θ-direction or z-direction except for the harmonic oscillation described by the wavenumber, the wave fields can be described by:

$$\Phi, H = \Gamma_{\Phi,H}\,(r)\,e^{ip\theta}e^{i(\xi z - \omega t)}, \tag{4}$$

where $\Gamma_{\Phi,H}\,(r)$ describe the wave field variation in r coordinate, ξ is the component of the complex vector wavenumber in the z-direction, since only propagation in the cylinder axis-direction is considered, p is referred to as the circumferential order which must be a whole number.

Recalling from Equation (1) and Hooke's law, the field variables such as displacements and stresses can be expressed in terms of potential functions, which can be numerically solved (see [11, 12, 13, 14] for more details on this subject).

On the other hand, the family of torsional modes results when only the u_θ displacement is assumed to exist ($u_r, u_z = 0$). Such a displacement field is obtained only if rotational potential function in z, $h_z \neq 0$. Then, for sake of brevity, only the expressions for u_θ, h_z, and the stress ($\sigma_{r\theta}$ as boundary condition), are used in forward to study the axisymmetric torsional modes as follows [14].

$$h_z\,(r) = K_1 J_p(\beta r), \qquad \beta^2 = \frac{\omega^2}{C_2^2} - \xi^2 \tag{5}$$

$$u_\theta = h_{z'}\,(r)\cos\,(p\theta)\,e^{i(\xi z - \omega t)}, \tag{6}$$

$$\sigma_{r\theta} = \mu\left[-\left(2h_{z''} - \beta^2 h_z\right)\right], \tag{7}$$

where J_p is the Bessel function of the first kind an order p, r is the cylinder radius, and K_1 is a constant. For the case of the axisymmetric modes, p=0, and by using the property of Bessel functions J_0' $(x) = -J_1(x)$, the corresponding u_θ can be expressed as:

$$u_\theta = -\frac{\partial h_z}{\partial r} = (K_1\beta)J_1\,(\beta r)\,e^{i(\xi z - \omega t)}. \tag{8}$$

The frequency equation for the torsional modes may be obtained by using the stress-free boundary condition Eq.(7) as follows:

$$\left[\beta^2 a^2 J_0\,(\beta a) - 2\beta a J_1\,(\beta a)\right] - \left[\beta^2 b^2 J_0\,(\beta b) - 2\beta b J_1\,(\beta b)\right] = 0. \tag{9}$$

where a and b are the inner and outer radius of the waveguide respectively . The fundamental torsional mode, the first root of Equation (9), is $\beta = 0$. But, this mode is not adequately described

by the Bessel equations [15]. So this particular mode is described by the RHS relation expressed in Eq. (5) which will be used to obtain the phase velocity of $T(0,1)$.

$$V_p = \frac{\omega}{\xi} = C_2 = \sqrt{\frac{D_{66}}{\rho}} \tag{10}$$

where D_{66} belongs to the lineal elasticity matrix of an isotropic specimen. Eq. (10) shows that $T(0,1)$ propagates at a constant phase velocity equivalent to the bulk shear velocity of the material.

2 The Acoustoelasticity Effect in T(0,1) mode

The acoustoelasticity effect in mechanics establishes the mathematical relationship between ultrasonic bulk velocities and mechanical stresses in the studied material. In this sense, the acoustoelasticity establishes five elastic constants to describe the relation between stress and bulk wave velocity for isotropic materials subject to uniaxial stress; the second order elastic constant, Lamé constants (λ, μ) and the third order elastic constants (TOEC), Murnaghans constants (m, n, l), in our case. The TOEC highly depend on the material processing, such as casting, rolling, or drawing.

Now, acoustoelasticity in [16], it is tackled by replacing the elastic constants (second order) in the stiffness tensor with effective elastic constants (EECs) to produce a modified elasticity matrix which terms consider the influence of stress. In particular, the term D_{66} is re-expressed in EEC as:

$$D_{66} = \mu + \frac{\sigma}{E}\left[3\mu + \frac{n}{4} + (1-2\nu)\left(\lambda + m - \frac{n}{4}\right)\right] \tag{11}$$

where E is the Youngs modulus, ν is the Poisson ratio and σ is the stress (positive for tension and negative for compression stresses). On the other hand, in [6] a first order approximation, considering finite deformation theory and third-order terms, for the acoustoelastic shear velocity propagating in the same direction as the applied stress is stated as follows:

$$C_2 = \sqrt{\frac{\mu}{\rho}}\left\{1 + \frac{\sigma}{2\mu\,(3\lambda + 2\mu)}\left(4\lambda + 4\mu + m + \frac{\lambda n}{4\mu}\right)\right\}. \tag{12}$$

So, based on the result expressed by Eq.(10) and the analytical models of the acoustoelastic shear velocity expressed by Eqs.(11)-(12) two approximate expressions for calculating the stressed phase velocity of the $T(0,1)$, are given by:

$$V^{\sigma}{}_{T(0,1)} = \sqrt{\frac{\mu}{\rho}}\left\{1 + \frac{\sigma}{2\mu\,(3\lambda + 2\mu)}\left(4\lambda + 4\mu + m + \frac{\lambda n}{4\mu}\right)\right\}. \tag{13}$$

$$V^{\sigma}{}_{T(0,1)} = \sqrt{\frac{\mu + \frac{\sigma}{E}\left[3\mu + \frac{n}{4} + (1-2\nu)\left(\lambda + m - \frac{n}{4}\right)\right]}{\rho}} \tag{14}$$

where $V^{\sigma}_{T(0,1)}$ is the velocity of the $T(0,1)$ mode when the torsional wave propagates under a stress (σ) along the cylinder axis, ρ is the mass density. Eq. (13) represents the approach named in figures as finite deformation, meanwhile Eq. (14) is the EEC approach. Expression inside curly brackets in Eq. (13) represents the stress influence in phase velocity of $T(0,1)$.

Clearly, the new expression for the phase velocity of the $T(0,1)$ depends on the second and third order elastic constants and the applied stress. In addition, in absence of dispersion, phase and group velocities are equal.

Although, $T(0,1)$ presents notable advantages as mentioned above (no dispersion and no leakage of energy through the fluid), is few sensible in term of velocity change to the acoustoelasticity effect. Experimental tests showed in [17], the smallest relatives changes associated with shear waves propagating perpendicular to the load and polarized perpendicular to the axial loads.

2.1 Sensitivity analysis of the stressed wave velocity of T(0,1) mode

In order to analytically estimate the variations of $T(0,1)$ velocity produced by uniform axial stress applied to the cylinder, the Murnaghan's and Lame's constants are required. In this work, it is used the reported values in [17]. Although the steel composition may be different among specimens, the close agreement of the reported TOEC values for different steels suggest that TOEC for steel

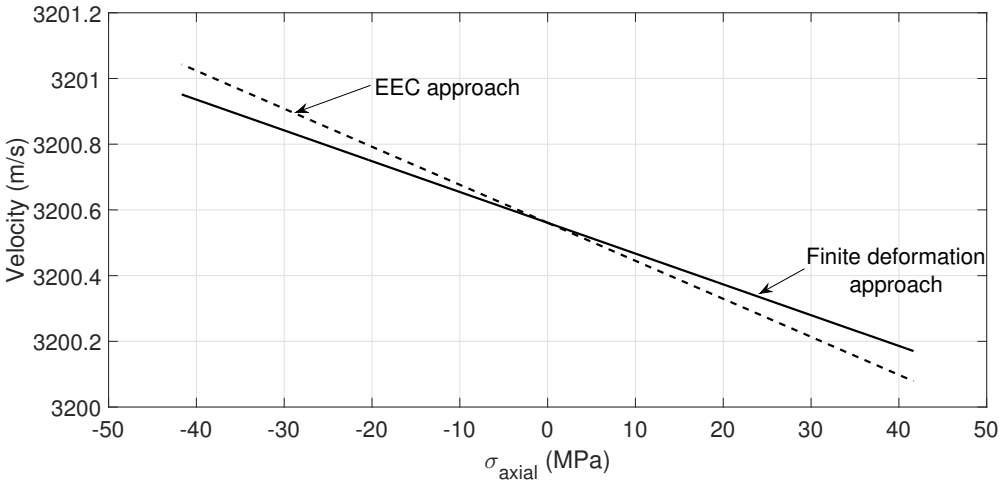

Figure 1: Velocity of T(0,1) for different stress levels (σ)

may be relatively independent of the specific composition. Here, $\rho = 7800kg/m^3$, $\mu = 79.9$ GPa, $\lambda = 115.8$ GPa, $l = -248$ GPa, $m = -623$ GPa, and $n = -714$ GPa are considered.

Fig. 1 shows the velocity of the fundamental torsional mode propagating in a specimen under different stress levels (-40 to 40 MPa). This plot is obtained by using Eqs.(13)-(14), where small velocity variations can be noted with a difference between the extreme cases of only 1 m/s. Comparing both models, the slope difference suggests an increasing gap in calculated velocity for greater stress values. For this reason, it is performed a FEM simulation to verify which approach provides a velocity value closer to the numerical model. Finally, as presented in Fig. 1 velocity magnitude increases for compression stresses and the opposite for tension stresses.

The practical implementation of a stress monitoring scheme based on variations of the phase velocity has some difficulties due to its small effect. Nevertheless, in order to determine the wave velocity change, a Time of Flight (TOF) estimation of the waves at different load conditions are performed.

Now, the TOF value in practice also consider the material elongation by applied load. Thus, the effect of the material elongation in the variation of the time of flight with respect to the stress-free condition has to be addressed. The variation of time of flight $\Delta(TOF)$ comparing with the stress-free condition is given by:

$$\Delta(TOF) = TOF_\sigma - TOF_0, \tag{15}$$

where TOF_σ is the time of propagation of $T(0,1)$ mode subject to an axial load, TOF_0 for the stress-free wave. TOF_σ is affected by the acoustoelasticity effect and the material elongation caused by the applied load as follows.

$$TOF_0 = \frac{l_0}{V_0}, \tag{16}$$

$$TOF_\sigma = \frac{l_0(1+\epsilon)}{V_\sigma}, \tag{17}$$

where l_0 is the original length of the material, ϵ is the strain after the load is applied, V_σ and V_0 are the phase velocity of $T(0,1)$ affected by the acoustoelasticity and stress-free respectively. Replacing Eqs (16)-(17) in Eq.(15) and using the constitutive relation yields.

$$\Delta(TOF) = \frac{l_0}{V_0}\left[\frac{V_0(1+(\sigma/E)) - V_\sigma}{V_\sigma}\right], \tag{18}$$

where E is the elasticity modulus. Based on the results presented in Fig. 1 and Eq. (18), it can be concluded that both effects (material elongation and acoustoelasticity) contribute to increase $\Delta(TOF)$ independently the kind of stress (tension or compression). Therefore, Eq. (18) suggests the use of the $\Delta(TOF)$ as a stress indicator in a stress guided wave monitoring scheme based on the propagation of $T(0,1)$. Two analytical expressions of fundamental torsional mode velocity propagating in a medium under mechanical stress are studied based on the acoustoelasticity effect. The expression depends on the material properties including the Lamé and the Murnaghans constants and the applied stress.

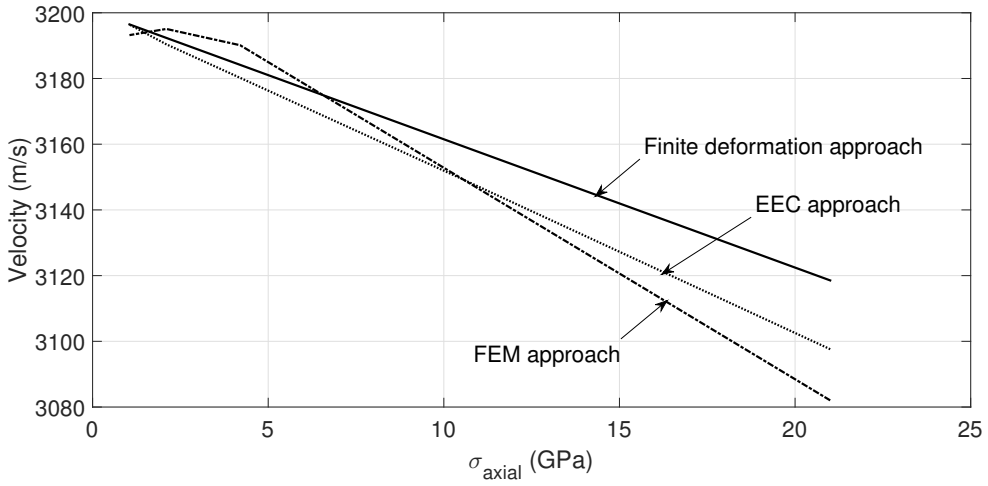

Figure 2: Phase velocity of T(0,1) for different stress levels (σ)

3 Finite Element Method approach

In order to investigate the Acoustoelastic effect in propagation of $T(0,1)$, FEM simulations are performed. A 3D FEM model was built representing a cylindrical specimen with a limited length to reduce the size of the FEM model and consequently the computational cost. A steel pipe of 1 inch schedule 40 (outer diameter: 33.4 mm and wall thickness: 3.38 mm) is modeled as a hollow cylinder with an axial length of 0.42 m. Changes in stress are configured varying the displacement of two constrains located at the left and right ends of the cylinder.

The material properties used for steel were assumed as follows: Density $\rho = 7830$ kg/m3, Young's modulus $(E) = 210$ GPa and Poisson's ratio $\nu = 0.3$. To ensure an adequate mesh refinement level, the minimum allowed inter-nodal length L_{min} is calculated. The lowest phase velocity C_T (i.e., transverse or shear wave speed), and consequently the shortest wavelength establishes the minimum permissible mesh size so spatial aliasing due to the finite element discretization does not occur [18]. Considering the frequency and the steel shear wave velocity, L_{min} is calculated as follows:

$$L_{min} = \frac{C_T}{n_{min} f_{max}} = \frac{\lambda_{min}}{n_{min}}, \tag{19}$$

where, n_{min} is the number of elements across the smallest wavelength of interest (assumed in this case as $n_{min} \geq 10$) [19], and f_{max} the maximum frequency of interest. Considering $n_{min} = 15$, $f_{max} = 50000$ Hz and $C_T = 3200$ m/s, the minimum element length results, approximately 6.66 mm. Therefore, seeds size of 3 mm can be considered as a sufficient mesh refinement.

In addition, the simulation is executed in two stages: first, uniaxial stress is applied as boundary displacement in both end sides of the cylinder. The stress and strain fields resulting are used as a predefined field in the next stage. The first stage is executed using a standard step and the next stage an explicit scheme. Explicit schemes are preferred as time marching process to simulate guided waves. So, an adequate integration time step Δt assures a more accurate solution. In general, simulation accuracy can be increased with increasingly smaller integration time steps but punished by a higher computational cost. So, the time step Δt has to be smaller than the critical time step Δt_{cr} which is the transit time of a dilatational wave through the smallest element in the model which can be calculated by [20].

$$\Delta t \leq \Delta t_{cr} = \frac{L_{min}}{C_L}, \tag{20}$$

where C_L is the velocity of the dilatational wave. A Δt of 5 $nsec$ meets these criterion (Considering $L_{min} = 3$ mm and $C_L = 5944$ m/s) and it is used to solve the model. A total of 9980 linear eight node brick element (C3D8) has been used with 52 elements around the circumferential section of the pipe. The torsional wave is produced by a shear load at the left end face of the cylinder by a 5 cycles Hanning-window tone burst of 50 kHz. The model is configured such as the torsional wave freely propagates along the z-axis.

4 Conclusions

As presented in Fig. 2 the estimation of the $T(0,1)$ velocity by EEC has a better agreement with the result of the FEM simulation. It is also observed a slope of approximately 6.1 m/s per GPa, which result in a low sensitivity expressed in time i.e. 90 nsec of $\Delta(TOF)$ per GPa if actuator and sensor are separated by 1 meter. Although some improvements can be done in sensitivity increasing the distance between T(0,1) generation and its capture. Clearly, the exploitation of the velocity change of T(0,1) with the purpose of waveguide stress monitoring has limitations for its low sensitivity.

References

[1] Fan Shi, Jennifer E. Michaels, and Sang Jun Lee. In situ estimation of applied biaxial loads with Lamb waves. *Journal of the Acoustical Society of America*, 133(2):677–687, 2013.

[2] Salim Chaki, Gilles Corneloup, Ivan Lillamand, and Henri Walaszek. Combination of Longitudinal and Transverse Ultrasonic Waves for In Situ Control of the Tightening of Bolts. *Journal of Pressure Vessel Technology*, 129(3):383, 2007.

[3] I. Bartoli, R. R. Phillips, S. Coccia, A. Srivastava, F. Lanza di Scalea, M. Fateh, and G. Carr. Stress dependence of ultrasonic guided waves in rails. *Journal of the Transportation Research Board*, 2159(2159):91–97, 2010.

[4] Feng Chen and Paul D. Wilcox. The effect of load on guided wave propagation. *Ultrasonics*, 47(1-4):111–122, 2007.

[5] P. W. Loveday, C. S. Long, and P. D. Wilcox. Semi-Analytical Finite Element Analysis of the Influence of Axial Loads on Elastic Waveguides. In D Moratal, editor, *Finite Element Analysis - From Biomedical Applications to Industrial Developments*, chapter 18, pages 439–454. InTech, 2012.

[6] S. Chaki and G. Bourse. Guided ultrasonic waves for non-destructive monitoring of the stress levels in prestressed steel strands. *Ultrasonics*, 49(2):162–171, 2009.

[7] S. Chaki and G. Bourse. Stress level measurement in prestressed steel strands using acoustoelastic effect. *Experimental Mechanics*, 49(5):673–681, 2009.

[8] C. Nucera and F. L. d. Scalea. Monitoring load levels in multi-wire strands by nonlinear ultrasonic waves. *Structural Health Monitoring*, 10(6):617–629, 2011.

[9] M. D. Beard, M. J. S. Lowe, and P. Cawley. Ultrasonic Guided Waves for Inspection of Grouted Tendons and Bolts. *Journal of Materials in Civil Engineering*, 15(June):212–218, 2003.

[10] Jabid E Quiroga, John Quiroga, Rodolfo Villamizar, Luis E Mujica, and Magda Ruiz. Guided Ultrasonic Wave for Monitoring Stress Levels in Pipelines. In *7th ECCOMAS Thematic Conference on Smart Structures and Materials (SMART 2015)*, pages 1–14, 2015.

[11] J. L. Rose. *Ultrasonic Waves in Solid Media*. Cambridge University Press, 2014.

[12] Erasmo Viola and Alessandro Marzani. Exact Analysis of Wave Motions in Rods and Hollow Cylinders.

[13] B.A Auld. *Acoustic Fields and Waves in Solids. Vol. II*. Wiley-Interscience, Stanford, California, 1 edition, 1973.

[14] K. Graff. Wave Motion in Elastic Solids,, 1975.

[15] A Armenakas, Denos Gazis, and G Herrmann. *Free Vibrations of Circular Cylindrical Shells*. Pergamon Press, london, 1 edition, 1969.

[16] Marc Duquennoy, Mohammadi Ouaftouh, Dany Devos, Frederic Jenot, and Mohamed Ourak. Effective elastic constants in acoustoelasticity. *Applied Physics Letters*, 92(24):1–3, 2008.

[17] D.M Egle and D.E Bray. Measurement of Acoustoelatic and Third-Order Elastic Constants for Rail Steel. *Journal of the Acoustical Society of America*, 60(3):27–30, 1976.

[18] SeJin Han. *Finite Element Analysis of Lamb Waves*. PhD thesis, Department of Aeronautical and Astronautical Engineering, 2007.

[19] Premesh Shehan Lowe, Ruth M. Sanderson, Nikolaos V. Boulgouris, Alex G. Haig, and Wamadeva Balachandran. Inspection of Cylindrical Structures Using the First Longitudinal Guided Wave Mode in Isolation for Higher Flaw Sensitivity. *IEEE Sensors Journal*, 16(3):706–714, 2016.

[20] Mickael Brice Drozdz. *Efficient Finite Element Modelling of Ultrasound Waves in Elastic Media*. PhD thesis, University of London, 2008.